APPLICATION OF GENETIC ALGORITHM AND ARTIFICIAL NEURAL NETWORK FOR PREDICTING THE SLUMP AND COMPRESSIVE STRENGTH OF ALKALI-ACTIVATED FLY ASH - GROUND GRANULATED BLAST FURNACE SLAG CONCRETE

Dinh Hoang Quan[1], Nguyen Thanh Bang[2]
1. Thuy Loi University
2. Vietnam Academy for Water Resources

Abstract: *This study presents the development of models for predicting the slump and compressive strength of Alkali-Activated Fly Ash-Ground Granulated Blast Furnace Slag (AAFS) concrete, utilizing genetic algorithm (GA) and artificial neural network (ANN) techniques. The models are based on four input parameters, include %Na_2O, %GGBS, W/S, and t_{paste}, and a total of 178 experiments were conducted to determine the slump and compressive strength of AAFS concrete. GA was used to optimize the hyperparameters of the ANN models, and to build the Mathematic model. The ANN models achieved R-squared values of 0.93 and 0.97 for slump and compressive strength, respectively, while the Mathematic model obtained R-squared values of 0.88 and 0.95 for slump and compressive strength, respectively. The results indicate that the compressive strength of AAFS concrete is significantly affected by %GGBS, %Na_2O, and W/S, while the slump is most influenced by t_{paste} and W/S. Furthermore, each t_{paste} value corresponds to two threshold values of W/S, with a slight change in W/S between the two thresholds resulting in a significant change in the slump. Similarly, each W/S value corresponds to two threshold values of t_{paste}, where a low t_{paste} value initially leads to a very low slump. However, beyond a certain threshold, the slump increases rapidly until it reaches an upper threshold value.*

Keywords: *ANN; GA; genetic algorithm; GEP; Geopolymer; alkali-activated concrete; AAFS concrete; slag; GGBS; fly ash; compressive strength; slump*

1. INTRODUCTION

Alkali-activated binders have been developed as a promising alternation to traditional Portland cement-based concrete. The chemical composition of this material differs from that of Portland cement, which is produced by grinding a mixture of clinker heated at high temperature with a small amount of gypsum or anhydrite. On the other hand, alkali-activated binders can be synthesized by exposing aluminosilicate materials to concentrated alkaline solutions, followed by curing at room temperature or slightly elevated temperatures. This approach enables the production of concrete with desirable properties while reducing the environmental impact of cement production [1].

The concept of alkali-activated materials was first explored in the 1940s by Purdon, who investigated the use of ground granulated blast furnace slag (GGBS) activated with sodium hydroxide solution [2]. In the 1990s, research began to focus on the use of fly ash and slag as primary raw materials for alkali-activated binders. These materials could be activated using a combination of alkaline activators, such as sodium silicate (Na_2SiO_3) and sodium hydroxide (NaOH) solutions [3] [4]. The resulting alkali-activated binders exhibited comparable or superior mechanical properties

Receipt Date: November 02th, 2022
Review Approval Date: November 21th, 2022
Publish Approval Date: December 03th, 2022

to Portland cement, as well as enhanced chemical resistance and durability [5]. Several countries, including Australia, China, India, and the United States, have invested significantly in the development and application of alkali-activated fly ash and slag-based concrete (AAFS). The use of AAFS materials improves the potential to reduce the carbon footprint of the concrete industry and contribute to sustainable construction practices [6]. Overall, the development of alkali-activated fly ash and slag binders represents a significant breakthrough in construction materials, providing an alternative to traditional Portland cement-based concrete that may improve performance, reduce environmental impact, and support sustainable development [5].

Predicting the slump and compressive strength of AAFS concrete is important for optimizing the mix design, controlling its quality during production, reducing the amount of physical testing required to assess its properties, and promoting its wider adoption in sustainable construction. Accurate predictions of these properties can improve the performance and durability of AAFS concrete, while minimizing the amount of materials used, saving time and money, and reducing the environmental impact of construction projects. Overall, the ability to predict the slump and compressive strength of AAFS concrete is critical for improving the understanding and predictability of this sustainable construction material, and promoting its use in a more sustainable and efficient manner. The use of machine learning techniques such as genetic algorithm (GA) and artificial neural network (ANN) for predicting the slump and compressive strength of AAFS concrete is a relatively recent development. Research into predicting the properties of traditional concrete using GA and ANN dates back several decades [7] [8] [9], but only in recent years have these techniques been applied to AAFS concrete. Subsequently, numerous studies have been conducted to assess the performance of GA and ANN models in predicting the slump and compressive strength of AAFS concrete, with many studies showing promising results [10] [11] [12]. These models have the potential to provide accurate predictions of AAFS concrete properties, while reducing the need for physical testing and improving the efficiency of the construction process. Bagheri et al. [13] utilized an ANN and GA to predict the compressive strength of boron-based alkali-activated fly ash-slag systems. Input variables included percentages of fly ash and slag, and ratios of B, Si, and Na in the alkali activator. Nagajothi and Elavenil [14] developed an ANN model for compressive strength of alkali-activated fly ash-slag concretes, using input parameters of slag-fly ash ratio and river sand–manufactured sand ratio. Faridmehr et al. [15] developed an ANN model for compressive strength of alkali-activated fly ash-slag self-compacting concretes, with input parameters of fly ash and slag contents and curing age. Shariatmadari et al. [16] used alkali-activated volcanic ash-slag-PC to stabilize sandy soil and developed ANN and evolutionary polynomial regression (EPR) models based on input parameters including replacements of volcanic ash and slag in PC, concentration of alkali activator, curing time, and curing temperature. Zhang et al. [17] proposed a chemical-informed machine learning model for compressive strength of alkali-activated fly ash-slag system with comprehensive input features. Kuang et al. [12] used a back propagation neural network (BPNN) to analyze and predict the slump and compressive strength of composite geopolymers formed by one or two combinations of slag, fly ash and metakaolin under different activator combinations. After comparing BPNN with random forest (RF) and k nearest neighbors (KNN) models, BPNN was found to have better performance. The BPNN model had higher accuracy, efficiency, and stronger promotion ability in predicting composite geopolymers. Xiaoyu Qin et al. [10] establishes ANN and alternating conditional

expectation (ACE) models to predict the compressive strength of alkali-activated slag (AAS) concrete using input parameters such as alkali concentration, modulus of activator, water/binder ratio, surface area of slag, and basicity index of slag. The models were found to have adequate accuracy, and the weight-influencing compressive strength of AAS was determined. It was concluded that an ANN model was more suitable for larger data sets, while ACE could be considered for smaller ones. However, these previous studies have some limitations. For example, some studies have been conducted with a relatively small sample size [15], while others have only evaluated the performance of the models under certain conditions[14] [15], which may not be representative of real-world scenarios. Additionally, the lack of standardized procedures for sample preparation, testing, and data analysis across different studies may affect the comparability of the results. However, the above studies still have limitations such as a relatively small sample size [15], not mentioning the effect of the activator solution [14] [15], not mentioning the effect of water [12] [16] and ignoring the influence of aggregates [10][12][15][16][17].

The composition of alkali-activated binder includes FA, GGBS, alkali solution (a mixture of sodium silicate liquid, sodium hydroxide and adding water), fine and coarse aggregates. These presources all affect the mechanical properties of AAFS concrete. Therefore, by using GA and ANN, this study aims to establish models to predict the slump and compressive strength of AAFS concrete, taking into account the influences of the activating solution, which consists of Na_2SiO_3, NaOH, and water. The characteristics of the activator solution that considered are $\%Na_2O$ (the mass ratio of Na_2O in the alkali-activated solution and total solids), Ms (the mass ratio of SiO_2 and Na_2O in the activated solution), and W/S (the mass ratio of total water and total solids). Additionally, the effects of fly ash and GGBS are considered, characterized by %GGBS (the mass ratio of GGBS and total binder). The effect of the aggregate is also considered through the average thickness of excess paste surrounding the aggregate, t_{paste}. The results of this research are expected to have significant implications for the construction industry, helping to improve the design and performance of AAFS concrete and contributing to the development of sustainable and eco-friendly construction materials.

2. FACTORS INFLUENCING THE SELECTION OF INPUT FEATURES

The selection of input features is a crucial step in ensuring the production of high-quality and consistent concrete. Various factors such as presources (FA, GGBS), activator solution (Na_2SiO_3, NaOH, and water), and aggregate (fine and coarse aggregates) can all impact the slump and compressive strength of concrete, especially under the same fabrication and curing conditions.

Previous studies have shown that the rate of fly ash replacement by GGBS significantly affects the physical and mechanical properties of AAFS concrete. Therefore, %GGBS was chosen as the binder characterization factor in this study. This should be calculated according to equation (1):

$$\%GGBS = \frac{mass\ of\ GGBS}{total\ mass\ of\ (GGBS+FA)}.100 \quad (1)$$

On the other hand, when studying the effect of the activator on the properties of AAFS concrete, it is necessary to separate the liquid-to-binder ratio into the water-to-solids ratio and the activator concentration for investigation. Because an increase in the liquid-to-binder ratio leads to an increase in the water-to-binder ratio (which usually reduces the strength of the concrete) and an increase in the activator concentration (which usually increases the strength of the concrete).

Furthermore, previous studies have typically used the mass ratio of sodium silicate to sodium hydroxide (SS/SH = 1.5-2.5) and the molarity of sodium hydroxide solution (8-

14M) as input parameters when preparing the alkali solution. However, these studies have used sodium silicate liquid with a silica modulus (SiO_2/Na_2O) of 2.0, while water glass produced in certain countries may have a silica modulus ranging from 1.5 to 2.7. Thus, this approach may not be practical since the type of water glass used can affect the quality of the concrete. To better quantify the preparation of the alkali solution, this study selected % Na_2O and Ms as input parameters. In which, % Na_2O represents the mass ratio of Na_2O in the alkali solution to the total binder, while Ms represents the mass ratio of SiO_2 to Na_2O in the alkali solution. By blending liquid sodium silicate, sodium hydroxide, and water in different proportions, the required Ms and % Na_2O can be achieved. However, the pre-study results on mortars indicate that Ms has less influence than %Na_2O and %GGBS [18]. Therefore, this study selected two characteristic factors, % Na_2O and water-to-solids ratio (W/S), to study the effect of the activator solution while keeping Ms constant at 1.2. These should be calculated according to equations (2)-(4):

$$\%Na2O = \frac{mass\ of\ Na2O\ in\ liquid}{total\ mass\ of\ solids\ (GGBS+FA+SiO2\ in\ liquid+Na2O\ in\ liquid\ )}.100 \quad (2)$$

$$W/S = \frac{total\ mass\ of\ water\ in\ liquid}{total\ mass\ of\ solids\ (GGBS+FA+SiO2\ in\ liquid+Na2O\ in\ liquid\ )} \quad (3)$$

$$\%Ms = \frac{mass\ of\ SiO2\ in\ liquid}{mass\ of\ Na2O\ in\ liquid} = constant = 1.2 \quad (4)$$

Additional, the influence of aggregate on the properties of concrete can be measured through the characteristic factor of average paste thickness, t_{paste}, which is determined by excess paste theory and particle packing density. According to this theory, in 1 m^3 of concrete, highly dense packing of fine and coarse aggregates can decrease the amount of paste filling the voids between aggregates, resulting in an increase in excess paste. This increases the distance between aggregate particles, reducing friction resistance and interlocking between aggregates, and ultimately improving the workability of fresh concrete. The volume of paste also significantly influences mechanical properties, dimensional stability, durability, and production cost of concrete. When studying the effect of aggregate on concrete properties, the volume of voids of aggregates and surface area should be considered. These values can be easily calculated using the modified Toufar's model.

Toufar's model is a packing model of aggregates that was proposed by Toufar et al. [19]. It assumes that aggregates are composed of spherical particles and that the packing arrangement is a regular close-packed structure. The model assumes that smaller particles are surrounded by four larger particles, and packing density is related to the diameter ratio by the factors k_d and k_s. The model calculates total packing density using equations that require information about initial packing density, relative density, and characteristic diameter of each class. The model was found to work best for larger diameter ratios but is unrealistic when a small amount of fine particles are added to coarse ones. The model was corrected by Goltermann et al. [20] as follows:

$$\emptyset_A = \frac{1}{\frac{y_1}{\emptyset_1}+\frac{y_2}{\emptyset_2}-y_2\left(\frac{1}{\emptyset_2}-1\right).k_d.k_s} \quad (5)$$

$$k_d = \frac{d_2-d_1}{d_2+d_1} \quad (6)$$

$$k_s = \begin{cases} 1-\frac{(1+4x)}{(1+x)^4} & if\ x \geq 0.4753 \\ 0.3881(x/0.4753) & if\ x < 0.4753 \end{cases} \quad (7)$$

$$x = \frac{y_1}{y_2}.\frac{\emptyset_2}{\emptyset_1(1-\emptyset_2)} \quad (8)$$

$$y_i = \frac{Grain\ volumn\ of\ class\ i}{Total\ grain\ volumn\ of\ 2\ classes} \quad (9)$$

$$\emptyset_i = \frac{Bulk\ density\ of\ class\ i}{Grain\ density\ of\ class\ i} \quad (10)$$

where Φ_A is the packing degree of aggregates. yi and Φi are the volume and packing density of class i, respectively. Factors k_d and k_s define the interaction between the particles. x is the ratio of the bulk volume of smaller particles to the void volume of larger particles. The characteristic diameter d_i of particles class i can be chosen as the sieve size for which there is 36.8% residue [20]. The model was developed for binary mixtures; however, it is possible to estimate the packing density of a blend containing more classes by combining a binary mixture with a third class in sequences. The modified Toufar's model is simple and easy to use, but its accuracy decreases as the number of size classes in the mixture increases.

According to modified Toufar's model, volume of voids of aggregate (V_{void}) and theoretical surface area (SSA) of aggregate was determined as follows:

$$V_{void} = V_{agg}.\frac{1-\emptyset_A}{\emptyset_A} \quad (11)$$

$$SSA = \sum_{i=1}^{n} n_i.\pi d_i^2 = \sum_{i=1}^{n} \frac{V_i}{\frac{1}{6}.\pi d_i^3}.\pi d_i^2 = 6\sum_{i=1}^{n} \frac{V_i}{d_i} \quad (12)$$

$$V_{agg} = \sum_{i=1}^{n} V_i \quad (13)$$

where n_i, d_i are the theoretical number and characteristic diameter of particles of aggregate class i, respectively; V_i and V_{agg} are the grain volume of aggregate class i and total aggregate, respectively.

Therefore, the average paste thickness, t_{paste}, is calculated using the equation (14):

$$tpaste = \frac{\text{Volumn of paste – Volumn of voids of aggregates}}{\text{Surface area of aggregates}}.10^6\ (\mu m) \quad (14)$$

3. METHODOLOGY

3.1. Genetic Algorithm

GA is a computational method inspired by natural evolution that is used to find solutions to optimization problems. In a GA, a population of potential solutions is generated and then evolved over successive generations through the application of selection, crossover, and mutation operators. The selection operator chooses the best individuals from the current population to be used as parents in the next generation. The crossover operator combines the genetic material of the selected parents to create new individuals, and the mutation operator introduces random changes to the genetic material of the new individuals. This process continues until a stopping criterion is met, such as a maximum number of generations or a satisfactory level of solution quality. The GA can be used to find optimal or near-optimal solutions to a wide range of problems, including optimization problems with non-linear, non-differentiable, or discontinuous objective functions (**Figure 1**). In this research, GA was used for hyperparameter optimization of ANNs and for developing mathematical models to predict slump and compressive strength of AAFS concrete.

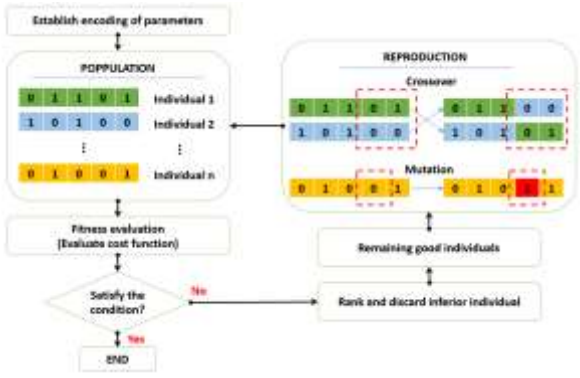

Figure 1: Evolution flow of Genetic Algorithm

3.2. Artificial Neural Network

ANNs are a type of machine learning algorithm that are loosely inspired by the structure and function of the biological neural networks in the human brain. ANNs consist of interconnected nodes, called neurons, that are organized into layers. The input layer receives the raw data, and then the data is processed through one or more hidden layers before arriving at the output layer. Each neuron in a layer receives inputs from the neurons in the previous layer, applies a mathematical transformation to the input, and then passes the output to the neurons in the next layer. During training, the weights of the connections between the neurons are adjusted so that the ANN can learn to make accurate predictions based on the input data. This is done by iteratively comparing the network's output to the desired output and using an optimization algorithm, such as backpropagation, in order to adjust the weights to minimize the error.

In this study, two ANN models were built with 4 inputs include %Na_2O, %GGBS, W/S and t_{paste}. Slump or compressive strength of AAFS concrete is the output of each model (**Figure 2**). Additional, GA was used to find the best combination of hyperparameters such as the hidden number size, activation functions, optimization and learning rate that result in the highest predictive accuracy for the ANN. GAsearchCV is a code library that uses GA to perform a grid search for hyperparameter tuning. It works by creating a population of hyperparameter combinations, which are encoded as chromosomes, and then evolving the population through several generations. The fitness of each chromosome is evaluated using K-fold cross-validation, with the ultimate goal of finding the hyperparameter set that yields the best average performance across all folds. The best-performing chromosomes are then selected for reproduction, creating a new generation of chromosomes with potentially better hyperparameter combinations. This process is repeated until a stopping criterion is met.

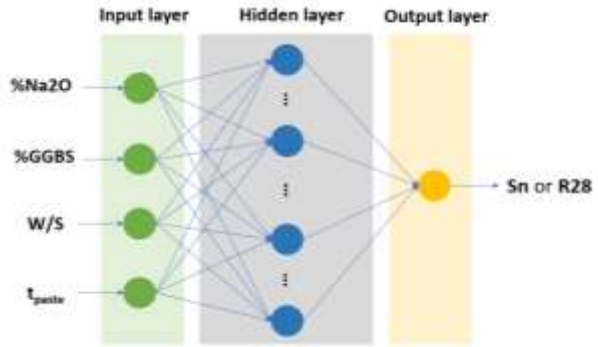

Figure 2: Neural network with 4 inputs, 1 output and a single hidden layer

3.3. Mathematic models

Mathematic (MAT) models were built with the help of Gene Expression Programming (GEP). This is a type of genetic programming that involves the use of an algorithm to evolve computer programs. The goal of GEP is to automatically discover a mathematical expression that can predict a particular output variable based on a set of input variables. The GEP algorithm works by generating an initial population of random programs (mathematical expressions) and then evolving them over a number of generations using a process of selection, recombination, and mutation. During each generation, the programs that perform the best (i.e., those that come closest to predicting the actual values of slump and compressive strength) are selected to be "parents" of the next generation. These parents are then recombined and mutated to create a new population of offspring programs, which are then evaluated to determine their fitness. The process continues for a number of generations, with the hope that the fittest programs in the final generation will provide an accurate mathematical model for predicting the output variables based on the input variables [21]. **Figure 3** shows an example of evolution of Gene Expression Programming.

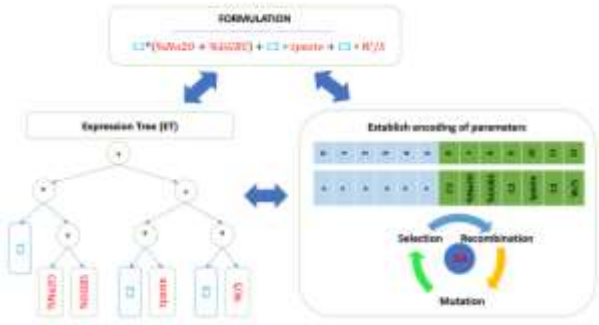

Figure 3: Example of evolution of Gene Expression Programming

4. MATERIALS AND EXPERIMENT

4.1. Materials

- *Fly ash (FA):* Most of the thermal power plants in Vietnam uses poor quality coal, resulting in the high LOI fly ash products (LOI>6%). Therefore, research on the use of FA with a high LOI content (this FA is not allowed to be used as mineral additives for cement) will bring great economic benefits. In this inquiry, 03 types of F-class fly ash according to TCVN 10302:2014 were used as the first binder. Chemical constituents of them were identified by X-Ray fluorescence (XRF) and displayed in **Table 1**.

- *Ground granulated blast-furnace slag (GGBS):* GGBS was used as the second binder in this study. GGBS was obtained from Hoa Phat Steel Joint Stock Company with finesses and chemical constituents displayed in **Table 1**.

Table 1: Chemical Composition of FA and GGBS (percentage by weight)

Chemical oxide	FA from HP*	FA from PL*	FA from FO*	GGBS
SiO_2	49.31	47.45	53.48	36.15
Al_2O_3	21.68	20.55	28.84	10.59
Fe_2O_3	8.76	5.17	4.73	0.35
CaO	1.27	8.3	4.12	39.13
MgO	1.62	1.6	2.31	7.59
SO_3	0.42	0.81	0.32	1.47
K_2O	4.36	3.84	1.25	0.95
Na_2O	0.13	0.24	0.85	0.2
TiO_2	0.98	0.76	1.8	0.54
MnO	0.08	0.05	0.04	2.25
P_2O_5	0.13	0.14	0.26	<0.01
LOI	11.32	10.93	1.83	-
Specific gravity (g/cm^3)	2.24	2.24	2.15	2.85
Blaine fineness (cm^2/g)	2935	2863	3617	3503
** HP, PL, and FO represent the Hai Phong, Pha Lai, and Formosa thermal power plants, respectively.*				

- *Alkali-activated solution:* This study used sodium hydroxide (NaOH) in powder form of 99% purity and sodium silicate as a solution ($Na_2O.rSiO_2.nH_2O$), or called water glass, with 26.7%SiO_2, 9.84%Na_2O and 63.46%H_2O, by weight.

- *Aggregate:* Coarse aggregates with medium size (10-20 mm) and small size (5-10 mm) were taken from Hoa Binh crushed stone. Fine aggregate was Lo river sand with fineness modulus of 2.61. All these aggregate were satisfied the requirements of Vietnamese standards TCVN 7570:2006. Relative density and bulk density of these material were determined according to ASTM C127/C128 and ASTM C29/C29M, respectively. The basic properties of the aggregates are shown in **Table 2**.

Table 2: Physical properties of aggregates

Sieve Size (mm)	Cumulative % Retained		
	Sand	Coarse aggregates	
		(5-10mm)	(10-20mm)
40	0	0	0
20	0	0	8.6
10	0	5.5	67.8
5	0	98.5	98.8
2.5	11.2	100	100
1.25	25.5	100	100
0.63	48.1	100	100
0.315	78.7	100	100
0.14	97.3	100	100
0	100	100	100
Rodded Bulk density, ρ_o (kg/m^3)	1562	1449	1590
Relative density, ρ_a (kg/m^3)	2620	2680	2680
Packing degree, Φi	0.596	0.541	0.593
Characteristic Diameter, di (mm)	0.94	8.32	15.24

4.2. Experimental

- Mixing procedure, curing and testing of specimens:

The study conducted 178 mixtures to evaluate the slump and 28-day compressive strength of AAFS concrete. The dry mixing process of fly ash, slag, and aggregate lasted for 2 minutes to ensure uniformity. The mixture was then activated by adding an alkali activator, prepared 24 hours in advance, containing water glass, NaOH, and water, and then mixed for an additional 2 minutes. The slump test of fresh AAFS concrete was carried out according to the Vietnamese standard TCVN 3106:1993 (**Figure 4**). The fresh AAFS concrete was immediately cast into three cubic molds with a dimension of 150 mm for each mixture. The molded specimens were kept for 24 hours at ambient conditions, and then removed from the molds and cured in a water tank until the testing day. The compressive strength tests were conducted using a universal testing machine according to the Vietnamese standard TCVN 3118:1993 at the day 28th (**Figure 4**). To determine the compressive strength of concrete, the maximum and minimum compressive strength values are compared to the compressive strength of the average pellet. If the deviation is within 15%, the arithmetic mean of the three test results is calculated. If not, the maximum and minimum values are discarded, and the compressive strength is determined from the remaining specimens.



Figure 4: Measuring slump and 28-days compressive strength of AAFS concrete

- *Experimental results:*

Table 3 displays the composition of 178 mixtures for 1m^3 AAFS concrete, along with the corresponding experimental results for both slump and compressive strength.

Table 3: Composition of mixture for 1m^3 AAFS concrete and experimental results

ID	Composition of mixture for 1m^3 AAFS concrete								Input variables				Outputs	
	Fly ash	GGBS	Na_2SiO_3 (liquid)	NaOH (solid)	H_2O (extra)	Sand	C.A.1 (5-10)	C.A.2 (10-20)	$\%Na_2O$	%GGBS	W/S	t_{paste}	Sn (mm)	R28 (MPa)
0	290.3	72.3	115.7	18.1	86.1	615	351	818	6.0	20.0	0.385	50.9	130	38
1	259.9	65.0	103.7	16.2	91.2	634	361	843	6.0	20.0	0.422	33.8	100	30
2	173.3	173.3	89.8	14.0	100.6	761	0	1078	5.0	50.0	0.407	22.3	90	61.61
3	121.9	284.8	76.7	12.0	115.5	616	351	819	3.0	70.0	0.372	50.2	160	16.6
4	88.3	352.2	121.1	18.9	96.9	594	339	790	5.3	80.0	0.351	71.6	235	76.3
5	89.7	357.8	140.8	22.0	83.6	590	336	785	5.9	80.0	0.339	75.7	250	87.3
6	88.9	354.8	141.3	22.0	83.9	591	337	786	6.0	80.0	0.342	75.0	250	85.2
7	118.7	276.5	107.2	16.7	85.7	626	357	832	5.2	70.0	0.347	40.9	120	75.3
8	116.7	271.9	107.5	16.8	105.3	610	348	811	5.3	70.0	0.397	55.8	200	75.6
9	115.1	268.3	108.1	16.9	106.0	611	348	812	5.4	70.0	0.404	55.0	200	67.5
10	92.7	215.8	98.4	15.4	104.4	645	368	858	6.0	70.0	0.472	23.8	210	62.6
11	198.5	198.5	102.9	16.1	92.5	715	0	1066	5.0	50.0	0.356	40.3	145	64.51
12	171.9	171.9	89.3	13.9	103.1	737	0	1100	5.0	50.0	0.416	24.4	100	61.11
13	148.2	148.2	76.9	12.0	108.6	806	0	1090	5.0	50.0	0.475	6.2	40	57.97
14	175.7	175.7	71.1	11.1	114.8	735	0	1100	4.0	50.0	0.417	25.1	95	45.55
15	170.7	170.7	88.8	13.9	103.4	739	0	1101	5.0	50.0	0.419	23.6	95	62.89
16	201.2	201.2	104.3	16.3	93.7	684	0	1086	5.0	50.0	0.356	45.9	150	67.45
17	227.3	227.3	118.0	18.4	85.2	634	0	1076	5.0	50.0	0.316	67.9	5	71.32
18	229.0	113.7	89.0	13.9	102.8	730	0	1095	5.0	33.2	0.416	27.8	110	49.57
19	170.7	170.7	88.8	13.9	103.4	739	0	1101	5.0	50.0	0.419	23.6	105	61.54
20	171.9	171.9	89.3	13.9	103.1	737	0	1100	5.0	50.0	0.416	24.4	95	60.25
21	146.3	146.3	59.1	9.2	122.3	786	0	1115	4.0	50.0	0.500	6.2	85	36.25
22	171.9	171.9	89.3	13.9	103.1	737	0	1100	5.0	50.0	0.416	24.4	90	60.93
23	41.4	372.5	138.2	21.6	59.1	629	359	837	6.2	90.0	0.309	37.7	5	89.6
24	93.5	217.2	99.1	15.5	111.4	637	363	847	6.0	70.0	0.490	30.5	200	62.5
25	30.1	270.7	57.1	8.9	123.8	664	379	883	3.0	90.0	0.489	7.8	75	4.7
26	223.8	223.8	116.0	18.1	84.4	666	0	1057	5.0	50.0	0.316	60.8	5	70.78
27	224.8	149.6	119.5	18.6	84.3	616	351	819	6.0	40.0	0.374	50.0	130	60

ID	Composition of mixture for 1m³ AAFS concrete								Input variables				Outputs	
	Fly ash	GGBS	Na_2SiO_3 (liquid)	NaOH (solid)	H_2O (extra)	Sand	C.A.1 (5-10)	C.A.2 (10-20)	$\%Na_2O$	%GGBS	W/S	t_{paste}	Sn (mm)	R28 (MPa)
28	226.7	226.7	117.6	18.3	85.5	636	0	1076	5.0	50.0	0.316	67.4	10	70.78
29	172.0	172.0	124.3	19.4	80.6	729	0	1097	6.7	50.0	0.398	27.8	95	73.67
30	120.6	180.9	96.0	15.0	98.8	774	0	1112	6.0	60.0	0.463	10.1	80	63.98
31	148.2	148.2	76.9	12.0	108.6	806	0	1090	5.0	50.0	0.475	6.2	50	55.56
32	106.4	248.7	113.3	17.7	104.6	618	352	822	6.0	70.0	0.434	47.9	200	69.5
33	116.9	272.5	89.2	13.9	116.4	612	349	814	4.5	70.0	0.403	53.5	215	50.7
34	171.9	171.9	89.3	13.9	103.1	737	0	1100	5.0	50.0	0.416	24.4	100	62.72
35	161.3	242.0	81.5	12.7	108.8	695	0	1091	4.0	60.0	0.365	40.9	135	60.09
36	180.2	120.2	95.7	14.9	98.5	768	0	1107	6.0	40.0	0.463	13.4	90	54.44
37	201.2	201.2	81.4	12.7	108.5	690	0	1087	4.0	50.0	0.365	43.5	155	56.11
38	226.7	226.7	91.7	14.3	102.1	642	0	1077	4.0	50.0	0.324	64.3	15	57.29
39	120.6	180.8	61.1	9.5	121.3	782	0	1116	4.0	60.0	0.486	7.1	65	38.07
40	100.2	234.4	106.7	16.7	97.5	637	363	846	6.0	70.0	0.431	31.2	150	67.4
41	227.3	227.3	117.8	18.4	85.3	634	0	1076	5.0	50.0	0.316	67.9	10	71.32
42	229.0	113.7	89.0	13.9	102.8	730	0	1095	5.0	33.2	0.416	27.8	105	51.2
43	146.3	146.3	59.1	9.2	122.3	786	0	1115	4.0	50.0	0.500	6.2	90	36.76
44	170.7	170.7	88.8	13.9	103.4	739	0	1101	5.0	50.0	0.419	23.6	105	61.99
45	161.3	242.0	81.5	12.7	108.8	695	0	1091	4.0	60.0	0.365	40.9	150	57.96
46	172.0	172.0	89.2	13.9	103.2	737	0	1100	5.0	50.0	0.416	24.4	105	58.01
47	150.4	150.4	60.9	9.5	121.2	779	0	1113	4.0	50.0	0.486	8.7	75	36.81
48	282.8	70.5	112.7	17.6	92.0	615	351	818	6.0	20.0	0.405	50.6	170	36
49	198.5	198.5	102.9	16.1	92.5	715	0	1066	5.0	50.0	0.356	40.3	135	68.31
50	180.2	120.2	95.7	14.9	98.5	768	0	1107	6.0	40.0	0.463	13.4	95	56.29
51	120.6	180.8	61.1	9.5	121.3	782	0	1116	4.0	60.0	0.486	7.1	70	39.98
52	296.2	32.9	105.0	16.4	77.5	641	365	852	6.0	10.0	0.383	27.6	15	15.5
53	161.3	242.0	81.5	12.7	108.8	695	0	1091	4.0	60.0	0.365	40.9	140	59.92
54	258.5	64.2	102.9	16.1	83.5	642	366	854	6.0	20.0	0.403	26.4	50	35
55	227.3	227.3	118.0	18.4	85.2	634	0	1076	5.0	50.0	0.316	67.9	5	72.74
56	251.9	63.2	100.5	15.7	88.1	642	366	854	6.0	20.0	0.421	26.0	100	32.5
57	138.9	207.8	63.0	9.8	129.9	630	359	838	3.2	60.0	0.453	37.0	180	8.4
58	207.4	207.4	119.9	18.7	83.5	670	0	1082	5.5	50.0	0.341	52.0	200	74.33
59	89.9	210.9	96.0	15.0	109.0	645	368	858	6.0	70.0	0.493	23.6	195	61.1
60	148.2	148.2	76.9	12.0	108.6	806	0	1090	5.0	50.0	0.475	6.2	45	54.18

ID	Composition of mixture for 1m³ AAFS concrete								Input variables				Outputs	
	Fly ash	GGBS	Na_2SiO_3 (liquid)	NaOH (solid)	H_2O (extra)	Sand	C.A.1 (5-10)	C.A.2 (10-20)	$\%Na_2O$	%GGBS	W/S	t_{paste}	Sn (mm)	R28 (MPa)
61	305.5	33.9	108.3	16.9	79.5	632	360	841	6.0	10.0	0.382	34.9	40	15
62	240.8	160.6	81.1	12.7	108.3	685	0	1084	4.0	40.0	0.365	46.1	155	53.15
63	227.3	227.3	117.8	18.4	85.3	634	0	1076	5.0	50.0	0.316	67.9	10	72.74
64	155.4	155.4	71.4	11.1	114.4	769	0	1109	4.5	50.0	0.465	12.5	85	49.89
65	97.5	227.1	103.5	16.2	95.1	644	367	857	6.0	70.0	0.433	24.3	90	68.2
66	171.9	171.9	89.3	13.9	103.1	737	0	1100	5.0	50.0	0.416	24.4	105	58.01
67	198.5	198.5	102.9	16.1	92.5	715	0	1066	5.0	50.0	0.356	40.3	140	67.45
68	240.8	160.6	81.1	12.7	108.3	685	0	1084	4.0	40.0	0.365	46.1	160	52.69
69	288.6	32.1	102.3	16.0	82.4	641	366	853	6.0	10.0	0.401	26.9	40	10
70	171.9	171.9	89.3	13.9	103.1	737	0	1100	5.0	50.0	0.416	24.4	100	56.28
71	205.1	136.4	108.9	17.0	104.1	618	352	821	6.0	40.0	0.443	48.6	220	51
72	175.7	175.7	71.1	11.1	114.8	735	0	1100	4.0	50.0	0.417	25.1	100	47.1
73	227.3	227.3	118.0	18.4	85.2	634	0	1076	5.0	50.0	0.316	67.9	10	69.05
74	114.5	230.5	89.6	14.0	103.5	744	0	1105	5.0	66.8	0.416	21.1	85	61.12
75	49.0	275.6	76.8	12.0	115.3	649	370	863	3.0	85.0	0.456	20.5	120	3.5
76	171.9	171.9	89.3	13.9	103.1	737	0	1100	5.0	50.0	0.416	24.4	90	61
77	171.9	171.9	89.3	13.9	103.1	737	0	1100	5.0	50.0	0.416	24.4	90	62.15
78	172.0	172.0	89.2	13.9	103.2	737	0	1100	5.0	50.0	0.416	24.4	105	60.93
79	155.4	155.4	71.4	11.1	114.4	769	0	1109	4.5	50.0	0.465	12.5	95	49.77
80	161.3	242.0	128.6	20.1	78.5	683	0	1088	6.0	60.0	0.347	45.9	150	81.58
81	173.3	173.3	89.8	14.0	100.6	761	0	1078	5.0	50.0	0.407	22.3	95	61.05
82	166.0	203.2	119.1	18.6	103.9	605	345	805	6.1	55.0	0.424	60.6	240	68.5
83	150.4	150.4	78.0	12.2	110.1	775	0	1111	5.0	50.0	0.475	10.1	80	57.97
84	226.7	226.7	91.7	14.3	102.1	642	0	1077	4.0	50.0	0.324	64.3	10	60.18
85	172.0	172.0	124.3	19.4	80.6	729	0	1097	6.7	50.0	0.398	27.8	105	70.62
86	171.9	171.9	89.3	13.9	103.1	737	0	1100	5.0	50.0	0.416	24.4	110	61.89
87	120.6	180.9	96.0	15.0	98.8	774	0	1112	6.0	60.0	0.463	10.1	85	62.97
88	201.2	201.2	104.3	16.3	93.7	684	0	1086	5.0	50.0	0.356	45.9	165	68.31
89	169.6	206.4	90.0	14.0	97.4	629	358	836	4.7	55.0	0.371	38.0	80	60.7
90	207.4	207.4	119.9	18.7	83.5	670	0	1082	5.5	50.0	0.341	52.0	180	73.55
91	276.0	68.5	109.9	17.2	97.3	616	351	819	6.0	20.0	0.424	50.2	190	31
92	172.0	172.0	124.2	19.4	80.6	729	0	1097	6.7	50.0	0.398	27.7	100	73.67
93	324.2	36.0	114.9	17.9	84.6	615	350	818	6.0	10.0	0.382	51.2	140	17

ID	Composition of mixture for 1m³ AAFS concrete								Input variables				Outputs	
	Fly ash	GGBS	Na_2SiO_3 (liquid)	NaOH (solid)	H_2O (extra)	Sand	C.A.1 (5-10)	C.A.2 (10-20)	$\%Na_2O$	%GGBS	W/S	t_{paste}	Sn (mm)	R28 (MPa)
94	203.6	135.7	108.3	16.9	87.4	634	361	843	6.0	40.0	0.402	33.4	100	56
95	226.7	226.7	117.6	18.3	85.5	636	0	1076	5.0	50.0	0.316	67.4	10	67.68
96	95.4	222.9	101.5	15.8	107.6	637	363	846	6.0	70.0	0.472	31.2	220	62
97	104.0	241.6	97.3	15.2	110.5	627	358	834	5.4	70.0	0.442	39.4	170	71.4
98	171.9	171.9	89.3	13.9	103.1	737	0	1100	5.0	50.0	0.416	24.4	95	62.04
99	175.7	175.7	91.1	14.2	102.0	730	0	1098	5.0	50.0	0.407	27.0	90	58.64
100	272.5	67.9	108.6	16.9	72.6	641	365	852	6.0	20.0	0.364	27.3	0	37.5
101	180.2	120.2	60.9	9.5	120.9	775	0	1110	4.0	40.0	0.486	10.4	80	37.06
102	227.3	227.3	117.8	18.4	85.3	634	0	1076	5.0	50.0	0.316	67.9	10	69.05
103	120.6	180.9	96.0	15.0	98.8	774	0	1112	6.0	60.0	0.463	10.1	80	61.96
104	316.3	35.1	112.1	17.5	91.0	614	350	817	6.0	10.0	0.403	51.6	170	12
105	171.9	171.9	89.3	13.9	103.1	737	0	1100	5.0	50.0	0.416	24.4	90	61.09
106	240.8	160.6	128.0	20.0	78.1	674	0	1081	6.0	40.0	0.347	51.2	185	63.39
107	114.5	230.5	89.6	14.0	103.5	744	0	1105	5.0	66.8	0.416	21.1	85	66.59
108	172.0	172.0	124.2	19.4	80.6	729	0	1097	6.7	50.0	0.398	27.7	100	70.62
109	55.5	314.2	69.0	10.8	121.3	634	361	843	3.3	85.0	0.412	33.7	115	12.5
110	180.2	120.2	60.9	9.5	120.9	775	0	1110	4.0	40.0	0.486	10.4	90	35.26
111	118.3	275.6	106.9	16.7	104.7	609	347	810	5.2	70.0	0.390	56.6	190	68.7
112	157.5	157.5	63.7	9.9	119.4	767	0	1108	4.0	50.0	0.465	13.1	95	42.35
113	172.0	172.0	124.3	19.4	80.6	729	0	1097	6.7	50.0	0.398	27.8	90	68.42
114	226.7	226.7	117.6	18.3	85.5	636	0	1076	5.0	50.0	0.316	67.4	15	73.43
115	206.4	137.6	109.7	17.1	84.9	634	361	843	6.0	40.0	0.393	33.8	55	58
116	171.9	171.9	89.3	13.9	103.1	737	0	1100	5.0	50.0	0.416	24.4	95	58.65
117	223.8	223.8	116.0	18.1	84.4	666	0	1057	5.0	50.0	0.316	60.8	5	73.43
118	161.3	242.0	128.6	20.1	78.5	683	0	1088	6.0	60.0	0.347	45.9	145	75.73
119	150.4	150.4	78.0	12.2	110.1	775	0	1111	5.0	50.0	0.475	10.1	85	55.56
120	180.2	120.2	60.9	9.5	120.9	775	0	1110	4.0	40.0	0.486	10.4	85	35.62
121	265.0	66.0	105.6	16.5	78.6	641	366	853	6.0	20.0	0.384	27.0	20	39
122	138.6	207.5	78.9	12.3	120.2	628	358	835	4.5	60.0	0.446	38.8	185	49.8
123	207.4	207.4	119.9	18.7	83.5	670	0	1082	5.5	50.0	0.341	52.0	190	74.43
124	223.8	223.8	116.0	18.1	84.4	666	0	1057	5.0	50.0	0.316	60.8	5	67.68
125	240.8	160.6	128.0	20.0	78.1	674	0	1081	6.0	40.0	0.347	51.2	175	68.96
126	175.7	175.7	91.1	14.2	102.0	730	0	1098	5.0	50.0	0.407	27.0	105	61.61

ID	Composition of mixture for 1m³ AAFS concrete								Input variables				Outputs	
	Fly ash	GGBS	Na_2SiO_3 (liquid)	NaOH (solid)	H_2O (extra)	Sand	C.A.1 (5-10)	C.A.2 (10-20)	$\%Na_2O$	%GGBS	W/S	t_{paste}	Sn (mm)	R28 (MPa)
127	120.6	180.8	61.1	9.5	121.3	782	0	1116	4.0	60.0	0.486	7.1	70	39.32
128	333.7	37.1	118.3	18.5	78.0	614	350	817	6.0	10.0	0.361	51.7	85	22
129	155.4	155.4	71.4	11.1	114.4	769	0	1109	4.5	50.0	0.465	12.5	90	50.1
130	161.3	242.0	128.6	20.1	78.5	683	0	1088	6.0	60.0	0.347	45.9	130	76.9
131	298.8	74.2	119.0	18.6	79.1	615	351	818	6.0	20.0	0.363	50.9	105	39
132	201.2	201.2	104.3	16.3	93.7	684	0	1086	5.0	50.0	0.356	45.9	160	64.51
133	229.0	113.7	89.0	13.9	102.8	730	0	1095	5.0	33.2	0.416	27.8	120	47.79
134	171.9	171.9	89.3	13.9	103.1	737	0	1100	5.0	50.0	0.416	24.4	100	60.62
135	137.7	206.0	63.2	9.9	130.4	631	359	839	3.1	60.0	0.458	36.5	185	5.3
136	146.3	146.3	59.1	9.2	122.3	786	0	1115	4.0	50.0	0.500	6.2	80	36.33
137	171.9	171.9	89.3	13.9	103.1	737	0	1100	5.0	50.0	0.416	24.4	95	58.89
138	200.9	133.9	106.8	16.7	90.6	634	361	843	6.0	40.0	0.413	33.5	100	56
139	157.5	157.5	63.7	9.9	119.4	767	0	1108	4.0	50.0	0.465	13.1	95	42.55
140	175.7	175.7	91.1	14.2	102.0	730	0	1098	5.0	50.0	0.407	27.0	110	61.05
141	157.5	157.5	63.7	9.9	119.4	767	0	1108	4.0	50.0	0.465	13.1	90	42.47
142	141.9	173.5	90.1	14.1	86.9	660	376	878	5.4	55.0	0.405	10.8	5	60.6
143	171.9	171.9	89.3	13.9	103.1	737	0	1100	5.0	50.0	0.416	24.4	105	60.09
144	191.8	128.5	102.2	15.9	89.6	644	367	856	6.0	40.0	0.421	25.1	75	56
145	172.0	172.0	89.2	13.9	103.2	737	0	1100	5.0	50.0	0.416	24.4	110	60.09
146	171.9	171.9	89.3	13.9	103.1	737	0	1100	5.0	50.0	0.416	24.4	90	59.06
147	114.5	230.5	89.6	14.0	103.5	744	0	1105	5.0	66.8	0.416	21.1	100	65.3
148	171.9	171.9	89.3	13.9	103.1	737	0	1100	5.0	50.0	0.416	24.4	100	63.8
149	274.0	68.7	109.3	17.1	79.7	633	361	842	6.0	20.0	0.380	34.2	50	40.5
150	297.6	33.1	105.5	16.5	85.3	633	361	841	6.0	10.0	0.402	34.7	70	12.5
151	216.2	143.8	114.9	17.9	93.2	616	351	820	6.0	40.0	0.403	49.6	170	58
152	98.9	230.7	105.2	16.4	119.3	619	353	824	6.0	70.0	0.492	46.8	240	60.5
153	180.2	120.2	95.7	14.9	98.5	768	0	1107	6.0	40.0	0.463	13.4	105	56.79
154	171.9	171.9	89.3	13.9	103.1	737	0	1100	5.0	50.0	0.416	24.4	95	57.51
155	118.4	276.0	88.8	13.9	115.8	611	348	813	4.4	70.0	0.396	54.4	190	54.4
156	100.3	233.5	113.8	17.8	84.3	644	367	856	6.4	70.0	0.406	24.8	80	73.4
157	240.8	160.6	128.0	20.0	78.1	674	0	1081	6.0	40.0	0.347	51.2	180	66.37
158	197.4	131.3	104.9	16.4	84.7	643	366	855	6.0	40.0	0.402	25.6	50	57.5
159	240.8	160.6	81.1	12.7	108.3	685	0	1084	4.0	40.0	0.365	46.1	145	47.92

ID	Composition of mixture for 1m³ AAFS concrete								Input variables				Outputs	
	Fly ash	GGBS	Na_2SiO_3 (liquid)	NaOH (solid)	H_2O (extra)	Sand	C.A.1 (5-10)	C.A.2 (10-20)	$\%Na_2O$	%GGBS	W/S	t_{paste}	Sn (mm)	R28 (MPa)
160	150.4	150.4	60.9	9.5	121.2	779	0	1113	4.0	50.0	0.486	8.7	65	36.53
161	187.1	124.7	99.5	15.5	95.1	644	367	856	6.0	40.0	0.443	25.1	100	52.5
162	150.4	150.4	60.9	9.5	121.2	779	0	1113	4.0	50.0	0.486	8.7	70	34.2
163	173.3	173.3	89.8	14.0	100.6	761	0	1078	5.0	50.0	0.407	22.3	95	58.64
164	89.1	355.3	120.7	18.8	96.6	593	338	789	5.2	80.0	0.347	72.3	230	78.2
165	266.4	66.8	106.3	16.6	85.7	634	361	842	6.0	20.0	0.402	33.9	65	35
166	201.2	201.2	81.4	12.7	108.5	690	0	1087	4.0	50.0	0.365	43.5	150	60.71
167	201.2	201.2	81.4	12.7	108.5	690	0	1087	4.0	50.0	0.365	43.5	155	58.15
168	172.0	172.0	124.2	19.4	80.6	729	0	1097	6.7	50.0	0.398	27.7	90	68.42
169	64.7	367.7	125.3	19.6	76.9	614	350	817	5.5	85.0	0.320	51.9	10	80.2
170	37.4	336.7	103.8	16.2	80.2	647	369	861	5.3	90.0	0.347	22.0	10	73.2
171	313.8	34.9	111.2	17.4	74.4	631	360	840	6.0	10.0	0.364	35.8	5	19
172	213.5	142.0	113.4	17.7	95.7	617	352	820	6.0	40.0	0.412	49.2	180	60
173	101.7	236.4	107.9	16.8	113.8	620	353	824	6.0	70.0	0.471	46.7	235	61.2
174	226.7	226.7	91.7	14.3	102.1	642	0	1077	4.0	50.0	0.324	64.3	5	59.53
175	39.0	350.7	91.5	14.3	117.1	617	352	820	4.6	90.0	0.406	49.2	180	55.3
176	175.7	175.7	71.1	11.1	114.8	735	0	1100	4.0	50.0	0.417	25.1	100	44
177	150.4	150.4	78.0	12.2	110.1	775	0	1111	5.0	50.0	0.475	10.1	80	54.18

5. MODELING RESULTS AND DISCUSSIONS

5.1. ANN models

Evolution of fitness over Generations for hyperparameters of ANN predicting of slump and compressive strength of AAFS concrete is shown in **Figure 5a and b**, respectively. The results demonstrated the effectiveness of using a GA in combination with cross-validation to optimize hyperparameters for an ANN model. The average fitness value is increasing from generation 0 to generation 10, with a few fluctuation. The standard deviation of the fitness values are decreasing, which indicates that the fitness values are becoming more consistent and the algorithm is converging towards a solution. As a result, the optimal hyperparameters and the accuracy of the two ANN models were determined as shown in **Table 4**.

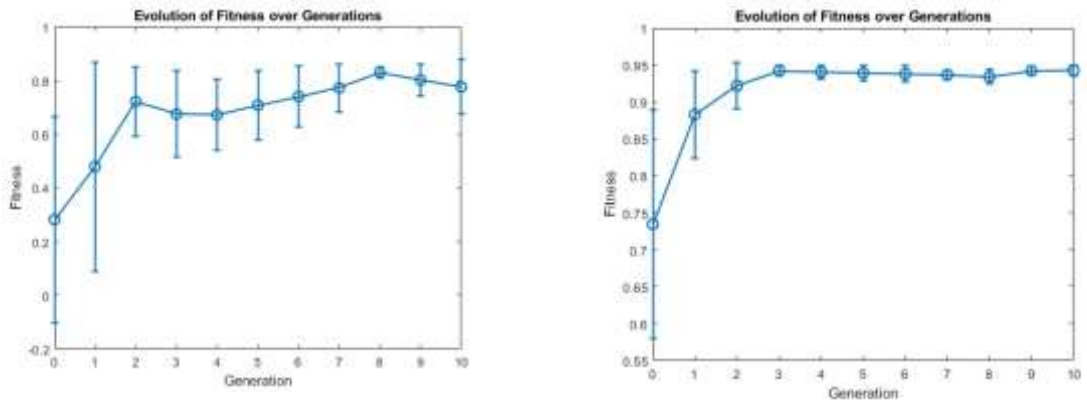

(a) (b)

Figure 5: Evolution of Fitness over Generations for hyperparameters of ANN predicting of (a) slump and (b) compressive strength of AAFS concrete

Table 4: The optimal hyperparameters and accuracy of ANNs

	The optimal hyperparameters				Training		Testing	
	Hidden layer size	Learning rate	Solver	Activation function	MSE	MAE	MSE	MAE
ANN for slump	(31,)	0.0654	Adam	tanh	267.2	11.1	221.7	10.5
ANN for compressive strength	(21,)	0.05454	Adam	tanh	12.8	2.7	7.6	2.2

Regression of ANN modeling for prediction of slump and 28-days compressive strength of AAS is given in **Figure 6 and 7**, respectively. R-squared score of 0.931 on the test data of slump and 0.974 for compressive strength indicated that the model explains 93.1% of the variability in the slump and 97.4% in the compressive strength of AAFS concrete. The results also showed that the model performed similarly on both the train and test data, with R-squared scores of 0.931 and 0.928 for slump, 0.956 and 0.974 for compressive strength, respectively. The mean squared error, mean absolute error, and root mean squared error were also very low, indicating that the models are highly accurate in predicting the slump and compressive strength of AAFS concrete (**Table 4**).

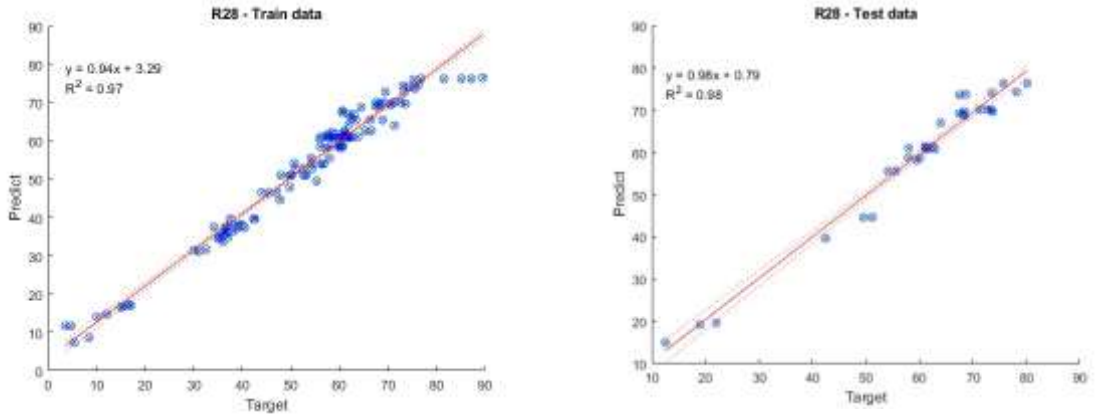

(a) (b)

Figure 6: Regression of ANN modeling for prediction of 28-days compressive strength of AAFS concrete. (a) Training. (b) Testing

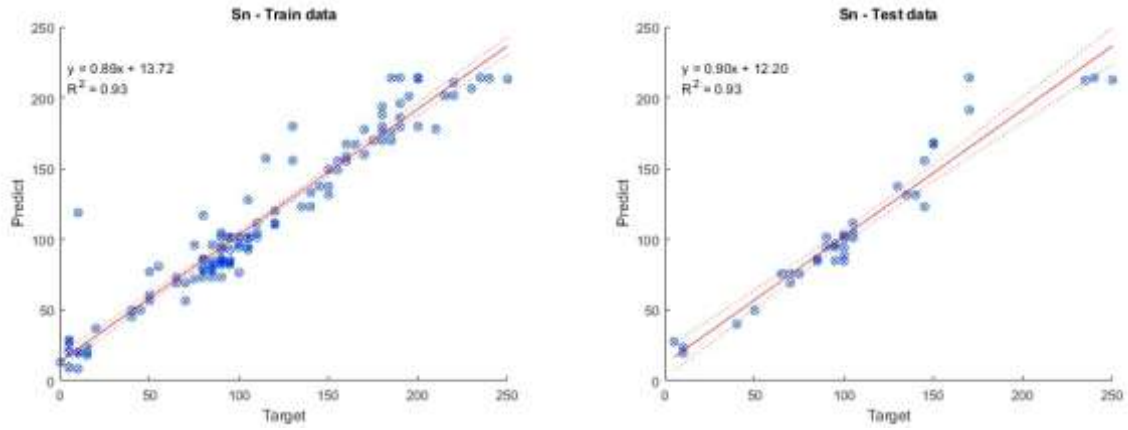

(a) (b)

Figure 7: Regression of ANN modeling for prediction of slump of AAFS concrete. (a) Training. (b) Testing

Permutation importance technique was used for evaluating the effect of input factors on the slump and compressive strength of AAFS concrete. This technique measures the contribution of each feature by retraining the model after permuting the values of the feature one at a time. The decrease in model performance resulting from each permutation is used to calculate the importance score of the feature. This approach provides a more reliable measure of feature importance, as it takes into account the actual contribution of each feature to the model's performance. The results shown in **Figure 8** indicate that the input variables in both models have different levels of importance in predicting the output variables of compressive strength and slump of AAFS concrete. In the compressive strength model, the most important feature is %GGBS, followed by %Na_2O, W/S, and t_{paste}. While in the slump model, t_{paste} and W/S has more significant impacts on the slump than %GGBS and %Na_2O. These results highlight different factors that affect the compressive strength and slump of AAFS concrete. The compressive strength is significantly affected by the GGBS utilization rate, concentration of alkaline solution and water-to-solid ratio, while the slump is most affected by the excess paste thickness and water-to-solid ratio. Understanding these differences help optimizing the mix design for specific performance requirements.

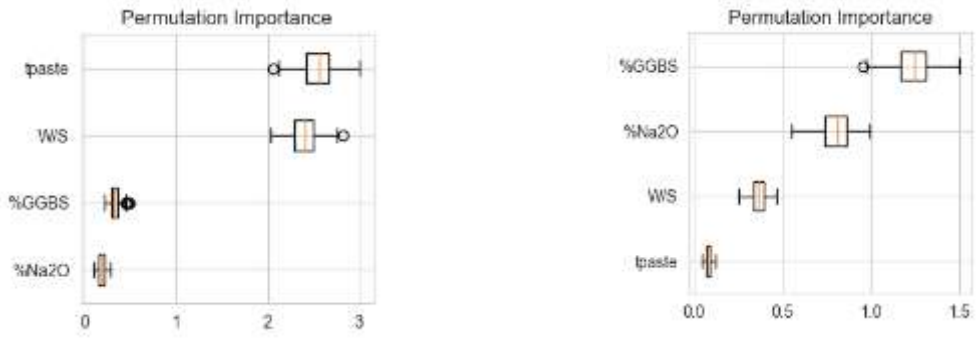

(a) (b)

Figure 8: Permutation importance of 4 inputs in ANN models for predicting (a) the slump, (b) compressive strength of AAFS concrete

The contour plots in Figure 9 illustrate the effects of three principal effective input parameters (%GGBS, %Na_2O, and W/S) on the compressive strength of AAFS concrete. These plots were created by varying two factors while keeping the other factors constant at their mean values. For instance, in the contour plots of the effect of %GGBS and %Na_2O on compressive strength, %GGBS was varied from 10% to 90%, %Na_2O was varied from 3 to 6.7%, while W/S and t_{paste} were kept constant at 0.41 and 27.8, respectively. According to Figure 4a and b, it appears that %GGBS has a stronger effect on the compressive strength of AAFS concrete when it is less than 40%. When %GGBS is high, its effect becomes less significant compared to %Na_2O and W/S. The less value of replacing fly ash with blast furnace slag, the less formation of gel-like C-(A)-S-H phases that are responsible for the initial strength development of AAFS concrete in room temperature curing. Additionally, %Na_2O and W/S can become more influential at high %GGBS because they can affect the degree of reaction and the availability of alkali ions in the solution. When %Na_2O is 3%, the intensity (i.e., compressive strength) is very low, which suggests that there is not enough alkali ions available to activate the reaction and form the required C-(A)-S-H phases responsible for initial strength development. However, it increases rapidly when %Na_2O increases to 4.5%. As %Na_2O continues to increase, the effect on compressive strength becomes less significant. This suggests that other factors, such as %GGBS and W/S, may become more influential at higher %Na_2O levels. According to Figure 9b and c, it can be seen that W/S is inversely proportional to the compressive strength of AAFS concrete. The reason is that excess water in the concrete mixture can lead to a more porous and weaker concrete structure. This can cause a reduction in the overall strength and durability of the concrete.

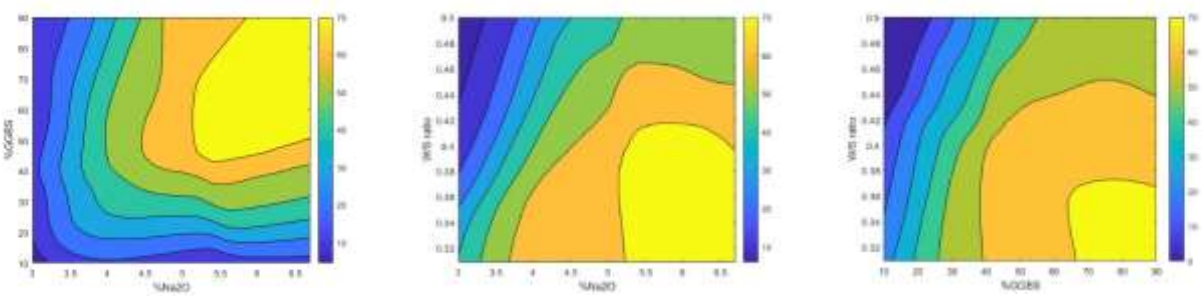

(a) (b) (c)

Figure 9: Effect of %GGBS, %Na_2O and W/S ratio on the compressive strength

Figure 10 presents contour plots that depict the impact of two key effective input parameters, namely t_{paste} and W/S, on the slump of AAFS concrete. In the plot, the two other inputs, $\%Na_2O$ and %GGBS, were kept constant at 5.0 and 50.0, respectively. The contour lines in the plot have a similar shape to a hyperbola, with each t_{paste} value corresponding to two thresholds of W/S values. Specifically, when W/S is significantly increased but has not yet surpassed the lower threshold, the slump of concrete is extremely low, indicating insufficient water for adequate flowability. However, when this threshold is exceeded, the slump of concrete increases rapidly from 40-60mm to 180-200mm until it reaches an upper threshold value beyond which the fluidity of the AAFS concrete does not significantly improve. These thresholds of W/S depend on the t_{paste} values, being small when t_{paste} is large and conversely. When t_{paste} is small, a large W/S ratio is needed to achieve the required slump.

On the other hand, the effect of t_{paste} on slump is comparable to that of W/S ratio. Initially, a low t_{paste} value leads to a very low slump, but beyond a certain threshold, the slump increases rapidly until it reaches an upper threshold value. The threshold values for t_{paste} are dependent on the W/S ratio, with smaller thresholds for larger W/S ratios and vice versa. These findings align with those of Li et al. [22], who also observed minimal impact of t_{paste} on slump at high W/B ratios, where the paste volume is high and aggregate particles are relatively low, resulting in low friction and bite forces. However, at medium W/B ratios, a small alteration in t_{paste} has a significant impact on slump. Optimizing t_{paste} is crucial for reducing cementitious material usage, while also enhancing the stability and durability of concrete.

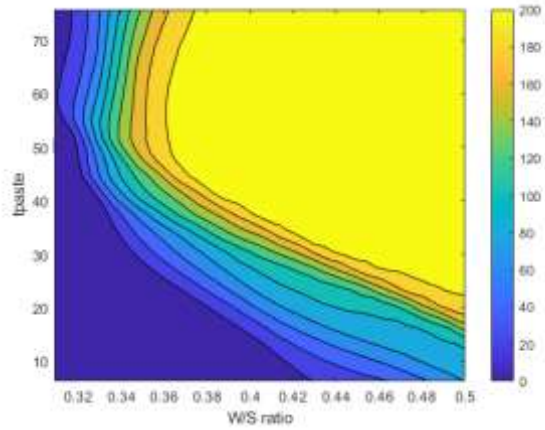

Figure 10: Effect of t_{paste} and W/S ratio on the slump

In conclusion, these contour plots show that %GGBS, $\%Na_2O$, and W/S are the three primary effective input parameters that cause impact on the compressive strength, while t_{paste} and W/S are key factors that affect the slump of concrete. The plots demonstrate that the optimal values for these input parameters depend on each other, and optimizing them can lead to stronger, more durable, and more stable concrete. These findings can guide the development of AAFS concrete with optimized properties for various construction applications.

5.2. Mathematic (MAT) models

Mathematic (MAT) models were built by using Gene Express Programming (GEP) for the prediction of two important properties, namely slump and compressive strength, of AAFS concrete. Four input parameters, include $\%Na_2O$, %GGBS, W/S, and t_{paste}, are considered for the development of predictive models. The proposed models for slump and compressive strength are formulated as follows:

$$Sn = \frac{[(tpaste - 1.344).tpaste]^{0.24}}{0.209^{(5.94^{W/S})}} - 4.265\frac{\%GGBS}{tpaste} + \frac{\%Na2O}{4.994(W/S - 0.33)} + \frac{tpaste(\%Na2O - 1.679)(tpaste.W/S - 21.781)}{\%GGBS}$$

$$R28 = \frac{\%GGBS}{6.988^{(W/S)}\left[(W/S)^{0.868} + \frac{1}{\%Na2O}\right]} - \frac{\%GGBS^2}{16.819 * \%Na2O} - \frac{(W/S - 0.387) * 16.64}{\%Na2O\ - 3.054} - \frac{tpaste}{\%GGBS} + \%Na2O + \%GGBS$$

The performance of the models is evaluated based on the R-square values, which are founded to be 0.88 and 0.95 for slump and compressive strength, respectively. The obtained results indicate that GEP can be used as an effective tool for the prediction of AAFS concrete's properties. The proposed models can be beneficial for the optimization of mix design and quality control of AAFS concrete, leading to the development of sustainable and durable concrete structures.

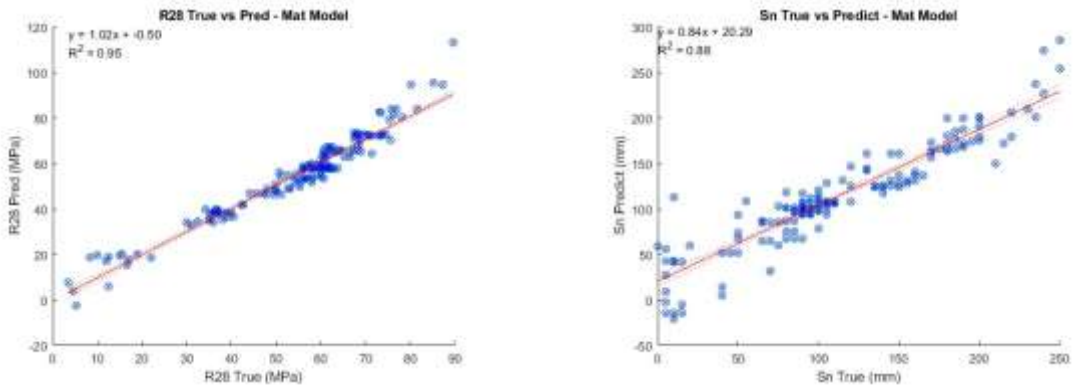

(a) (b)

Figure 11: Regression of MAT model for prediction of (a) compressive strength and (b) slump of AAFS concrete

Furthermore, the results as shown in **Figure 12** indicate that the input variables in both MAT models have different levels of importance in predicting the output variables of compressive strength and slump of AAFS concrete. It is shown that the compressive strength is significant affected by %GGBS, $\%Na_2O$ and W/S, while the slump is most affected by t_{paste} and W/S. These results are consistent with the ones obtained from the ANN models.

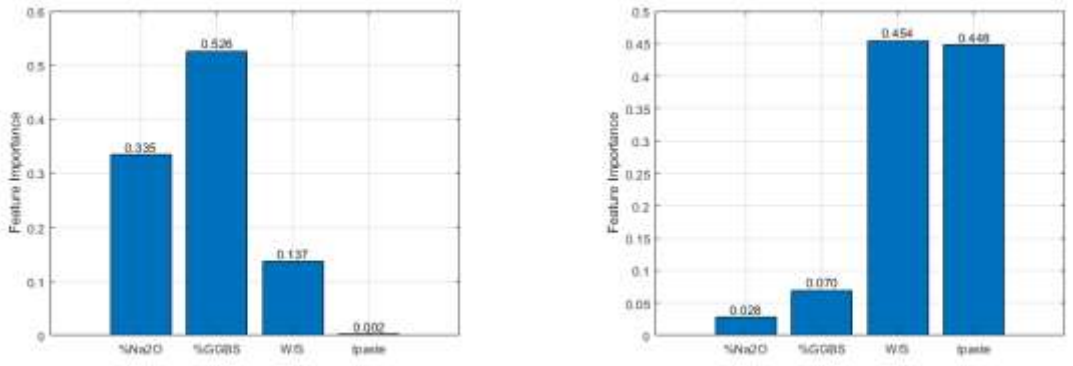

(a) (b)

Figure 12: Feature importance for MAT models (a) to predict compressive strength and (b) to predict slump of AAFS concrete

CONCLUSION

In this study, MAT and ANN models were developed to predict the slump and compressive strength of AAFS concrete using four input variables (%Na_2O, %GGBS, W/S, and t_{paste}). The effects of these variables on the target responses were evaluated and the following conclusions were drawn:

- Both models performed well in predicting the slump and compressive strength of AAFS concrete, in which the ANN model showing higher accuracy and the MAT model being more interpretable and intuitive.
- The study revealed the significant impact of paste thickness (t_{paste}) on the slump of AAFS concrete, and proposed a simple calculation for determining t_{paste} based on the modified Toufar's model and the excess paste theory.
- The compressive strength of AAFS concrete was found to be significantly affected by %GGBS, %Na_2O, and W/S, while the slump was mostly influenced by t_{paste} and W/S.
- The models also revealed that each t_{paste} value corresponds to two threshold values of W/S, with a small change in W/S between the thresholds leading to a significant change in the slump. Similarly, each W/S value corresponds to two threshold values of t_{paste}, with a low t_{paste} value initially causing a very low slump. However, beyond a certain threshold, the slump increases rapidly until it reaches an upper threshold value.

Overall, the developed models provide an useful tool for predicting the slump and compressive strength of AAFS concrete and can be used to optimize mix design and reduce experimental cost and time. The findings not only shed light on the importance of t_{paste} in controlling the slump of AAFS concrete but also provide valuable insights for further research in this field.

ACKNOWLEDGEMENT

We acknowledge the financial support provided by the Ministry of Science and Technology, Vietnam for the national project KC08.21/16-20, which has contributed significantly to our research work.

REFERENCES

[1] J. Davidovits, "Geopolymer: Inorganic polymeric new materials," *Journal of Thermal Analysis*, vol. 37, pp. 1633-1656, 1991.

[2] Purdon A.O., "The action of alkalis on blast furnace slag," *Journal of the Society of Chemical Industry*, vol. 59, pp. 191-202, 1940.

[3] Shao-Dong Wang, Karen L. Scrivener, P.L. Pratt, "Factors affecting the strength of alkali-activated slag," *Cement and Concrete Research*, vol. 24, no. 6, pp. 1033-1043, 1994.

[4] P. Krivenko, "Alkaline cements: terminology classification, aspects of durability, in: H. Justnes (Ed.), Proceedings of the 10th International Congress on the Chemistry of Cement, Gothenburg, Sweden, Amarkai and Congrex Göteborg, Gothenburg, Sweden, 1997, 4iv046, p. 6".

[5] Caijun Shi, Della Roy, Pavel Krivenko, Alkali-Activated Cements and Concretes, New York: Taylor & Francis, 2005.

[6] Ouellet-Plamondon C. , Habert G., "25 - Life cycle assessment (LCA) of alkali-activated cements and concretes," in *Handbook of Alkali-Activated Cements, Mortars and Concretes*, Woodhead Publishing, 2015, pp. 663-686.

[7] I.-C. Yeh, "Modeling of strength of high-performance concrete using artificial neural networks," *Cement and Concrete Research*, vol. 28, no. 12, pp. 1797-1808, 1998.

[8] Vinay Chandwani, Vinay Agrawal, Ravindra Nagar, "Modeling slump of ready mix concrete using genetic algorithms assisted training of Artificial Neural Networks," *Expert Systems with Applications*, vol. 42, no. 2, pp. 885-893, 2015.

[9] M.A. DeRousseau, J.R. Kasprzyk, W.V. Srubar, "Computational design optimization of concrete mixtures: A review," *Cement and Concrete Research*, vol. 109, pp. 42-53, 2018.

[10] Xiaoyu Qin, Qianmin Ma, Rongxin Guo, Zhigang Song, Zhiwei Lin, Haoxue Zhou, "Compressive Strength Prediction of Alkali-Activated Slag Concretes by Using Artificial Neural Network (ANN) and Alternating Conditional Expectation (ACE)," *Advances in Civil Engineering*, vol. 2022, p. 24, 2022.

[11] Tang, Y.X.; Lee, Y.H.; Amran, M.; Fediuk, R.; Vatin, N.; Kueh, A.B.H.; Lee, Y.Y., "Artificial Neural Network-Forecasted Compression Strength of Alkaline-Activated Slag Concretes," *Sustainability*, vol. 14, no. 9, p. 5214, 2022.

[12] Fenglan Kuang, Zhilin Long, Dumin Kuang, Xiaowei Liu, Ruiqi Guo, "Application of back propagation neural network to the modeling of slump and compressive strength of composite geopolymers," *Computational Materials Science*, vol. 206, 2022.

[13] Ali Bagheri, Ali Nazari, Jay Sanjayan, "The use of machine learning in boron-based geopolymers: Function approximation of compressive strength by ANN and GP," *Measurement*, vol. 141, pp. 241-249, 2019.

[14] Nagajothi, S., Elavenil, S., "Influence of Aluminosilicate for the Prediction of Mechanical Properties of Geopolymer Concrete – Artificial Neural Network," *Silicon*, vol. 12, p. 1011–1021, 2020.

[15] Faridmehr, I.; Nehdi, M.L.; Huseien, G.F.; Baghban, M.H.; Sam, A.R.M.; Algaifi, H.A., "Experimental and Informational Modeling Study of Sustainable Self-Compacting Geopolymer Concrete," *Sustainability*, vol. 13, no. 13: 7444, 2021.

[16] Nader Shariatmadari; Hadi Hasanzadehshooiili; Pooria Ghadir; Fatemeh Saeidi and Farshad Moharami, "Compressive Strength of Sandy Soils Stabilized with Alkali-Activated Volcanic Ash and Slag," *Journal of Materials in Civil Engineering*, vol. 33, no. 11, 2021.

[17] Lei V. Zhang, Afshin Marani, Moncef L. Nehdi, "Chemistry-informed machine learning prediction of compressive strength for alkali-activated materials," *Construction and Building Materials*, vol. 316, no. 126103, 2022.

[18] Hoang-Quan Dinh, Thanh-Bang Nguyen, "Composition of ground granulated blast-furnace slag and Composition of ground granulated blast-furnace slag and sodium hydroxide solution: multi-response optimization," *Vietnam Journal of Science, Technology and Engineering*, vol. 63, no. 1, pp. 21-29, 2021.

[19] W. Toufar,M. Born, E. Klose, "Beitrag zur optimierung der packungsdichte polydisperser korniger systeme," in *Freiberger Forschungsheft A*, vol. 558, VEB Deutscher Verlag fur Grundstoffindustrie, 1976, pp. 29-44.

[20] P. Goltermann, V. Johansen, L. Palbal, "Packing of aggregate: an alternative tool to determine the optimal aggregate," *ACI Materials Journal*, vol. 94, no. 5, pp. 435-443, 1997.

[21] Cândida Ferreira, "Gene Expression Programming: A New Adaptive Algorithm for Solving Problems," *Complex Systems*, vol. 13, no. 2, pp. 87-129, 2001.

[22] N. Li, C. Shi, Z. Zhang, D. Zhu, H-J Hwang, Y. Zhu, et al., "A mixture proportioning method for the development of performance-based alkali-activated slag-based concrete," *Cement Concr Compos*, vol. 93, p. 163–174, 2018.